

Optical Absorption and Photoconductivity in Barium Oxide*

W. W. TYLER† AND R. L. SPROULL
 Cornell University, Ithaca, New York
 (Received October 30, 1950)

Measurements of the optical absorption and photoconductivity in BaO single crystals are reported. The threshold photon energy for both processes is 3.8 eV, and the absorption constant at higher energies is at least 10^6 cm^{-1} . A second increase in the absorption constant begins at about 4.8 eV and is not accompanied by photoconductivity. The observed dependence of photoconductivity on temperature and electric field strength indicates space charge effects in limiting current flow. The onset of absorption at 3.8 eV is thought to be due to the production of excitons, with the accompanying photoconductivity due to thermal dissociation of excitons or exciton ionization of impurity centers.

I. INTRODUCTION

CATHODES coated with mixtures of barium oxide and strontium oxide have great practical importance, having been used for many years as low temperature sources of electrons in vacuum tubes. The aggregates of small oxide particles comprising the cathodes are not well understood, although much effort has been devoted to their study.¹ One aim of the present work was to approach an understanding of the oxide cathode by studying the fundamental electronic properties of a simpler system, a single crystal of BaO. Knowledge of the location and separation of energy bands in the BaO lattice and the identification of impurity levels should assist in an understanding of thermionic emission, activation, poisoning, and other phenomena of oxide-coated cathodes.

In addition to its practical importance as an electron emitter, BaO is of quite general interest. At present, very little is known about the electronic properties of crystals of the divalent alkaline earth oxide group. Most of the present theory of processes in ionic crystals has been developed² on the basis of studies of the properties of alkali halide crystals. This theory can be tested and perhaps influenced by an equivalent understanding of the properties of the divalent oxides.

II. PREPARATION OF CRYSTAL SAMPLES

Single crystals of the alkali halide group occur naturally or may be grown artificially with relative ease. The alkaline earth oxides do not occur naturally and are difficult to grow artificially because of their high melting temperatures and chemical activity at these temperatures. In addition, BaO is unstable in the atmosphere, combining with H₂O to form the hy-

droxide. This fact presents problems in the growth, manipulation, and study of the crystals.

The crystals used in the work presented here were all grown³ from the vapor phase at a temperature of approximately 1500°C. This method of growth produced clusters of small BaO crystals from which single crystals could be extracted or larger, multicrystalline plates cut with a high speed silicon carbide saw. The largest single crystals used in this work were approximate cubes with edges of the order of 1 mm. Preparation of the crystal samples and mounting of these samples for experimental work was done in a dry box desiccated by porous BaO or with a liquid nitrogen cold trap.

The growth of BaO crystals from pressed BaO powder is a purifying process. However, the chemical purity of the crystals obtained is still limited principally by the purity of the starting material.⁴ During growth, variable amounts of molybdenum are added to some crystals due to evaporation from the furnace heater. The total impurity content, estimated from spectroscopic analysis is at most 0.4 percent for the crystals used. Except for several crystals heavily dosed with molybdenum (Run 27), the major impurities are strontium (0.2 percent) and calcium (0.05 percent).

III. OPTICAL ABSORPTION MEASUREMENTS

Absorption measurements on single crystals and multicrystalline plates were made with the samples mounted in an airtight absorption cell with quartz windows. Mounting and sealing were done in the dry box. The ratio of light intensity passing through the cell windows and sample to that passing through the windows alone gives the transmittance of the sample. A Hanovia hydrogen discharge tube and a Bausch and Lomb quartz monochromator provided fairly continuous monochromatic radiation through the spectral region

* This work has received support from a Frederick Gardner Cottrell Grant by the Research Corporation and from the ONR.

† Now at the Knolls Atomic Power Laboratory of the General Electric Company, Schenectady, New York.

¹ See review articles by J. P. Blewett, *J. Appl. Phys.* **10**, 668, 831 (1939); **17**, 643 (1946); A. S. Eisenstein, *Advances in Electronics* (Academic Press, Inc., 1948), Vol. 1, pp. 1-64.

² N. F. Mott and R. W. Gurney, *Electronic Processes in Ionic Crystals* (Oxford University Press, 1940); F. Seitz, *The Modern Theory of Solids* (McGraw-Hill Book Company, Inc., New York, 1940).

³ Details of the method of growth will soon be published in *Rev. Sci. Instr.*

⁴ Utilizing seed crystals of cleaved MgO and purer BaO powder as raw material, W. C. Dash, in this laboratory, has recently obtained larger BaO crystals of higher purity. The above data on crystal size and purity pertain to the crystals used for the measurements reported subsequently. Checks using the purer crystals now available indicate that the results to be reported are to a large extent intrinsic to the BaO lattice and independent of impurity content.

from 4000Å to 2000Å. An RCA 1P28 photomultiplier tube and sensitive dc amplifier were used to detect light energy. The resolution of the system was such that the half-intensity width of the Hg 3650Å line was 70Å; the resolution improves for shorter wavelengths as the dispersion of the quartz prisms increases.

Figure 1 shows transmission data for a single crystal of BaO. Within the wavelength resolution the transmission cutoff was the same for samples of different impurity content from four different crystallizing runs. Absorption in BaO crystals begins quite abruptly at about 3.8 eV or 3250Å. Beyond 3100Å, the absorption constant is at least as great as 300 cm^{-1} . Crystals cannot be cleaved into thin enough specimens to measure the absorption constant in this region, so evaporated BaO films must be used. Figure 1 also shows a transmission curve for a MgO crystal.⁵ Studies of ultraviolet optical absorption in MgO were first reported by Brice and Strong.⁶ It is notable that even for thinner samples, the transmission cutoff for BaO is much sharper than for

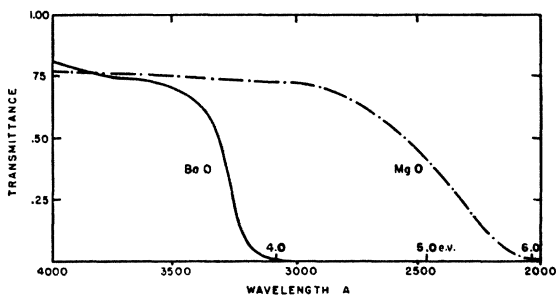


FIG. 1. Optical transmittance of BaO and MgO crystals. The BaO crystal is 0.38 mm thick. The MgO crystal is 1.2 mm thick.

MgO. For three MgO samples studied, the absorption constant at 2100Å is only about 15 cm^{-1} and may in part be due to impurity centers.⁷ As neither the MgO nor the BaO samples had optically polished surfaces, the relative values of transmittance in the 4000Å region are not significant.

The results of optical absorption measurements on BaO films have been reported.⁸ The threshold for absorption in films occurs at about 3.8 eV, in agreement with single crystal studies. Figure 2 shows the absorption constant as a function of wavelength. Taft and Dickey⁹ have confirmed location of the optical absorption edge in BaO at 3.8 eV by measuring the photoelectric emission from very thin metallic films deposited on the surface of BaO layers.

⁵ Obtained from the Norton Company, Niagara Falls, Ontario, Canada.

⁶ R. T. Brice and J. Strong, *Phys. Rev.* **47**, 255 (1935); *J. Opt. Soc. Am.* **25**, 207 (1935).

⁷ J. P. Molnar and C. D. Hartman, *Phys. Rev.* **79**, 1015 (1950).

⁸ W. W. Tyler, *Phys. Rev.* **76**, 1887 (1949).

⁹ E. A. Taft and J. E. Dickey, *Phys. Rev.* **78**, 625 (1950).

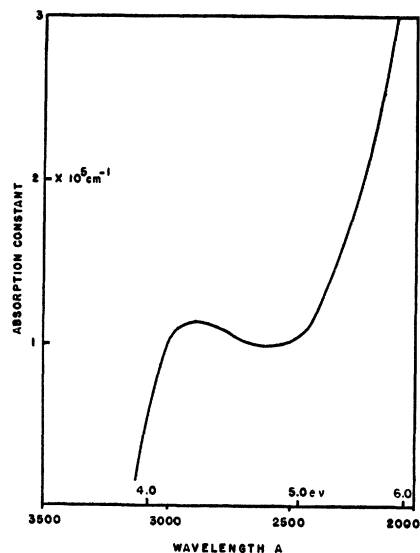


FIG. 2. Absorption constant of BaO as a function of wavelength. The curve represents the average of data from three thin films of BaO on quartz; the original data is from reference 8.

IV. PHOTOCONDUCTIVITY MEASUREMENTS

A. Direct Current Measurements

Preliminary measurements of photoconductivity in BaO crystals using steady-state dc detection methods have been reported.¹⁰ Although it had been shown by early workers¹¹ that single pulse ballistic measurements of photoconductivity were easier to interpret than steady-state measurements, it was felt that the BaO crystals available were too small for successful ballistic-type measurements. For the dc measurements, the crystal was mounted in vacuum between nickel electrodes across which a dc potential of about 300 v was applied. The crystals used in the dc experiments were

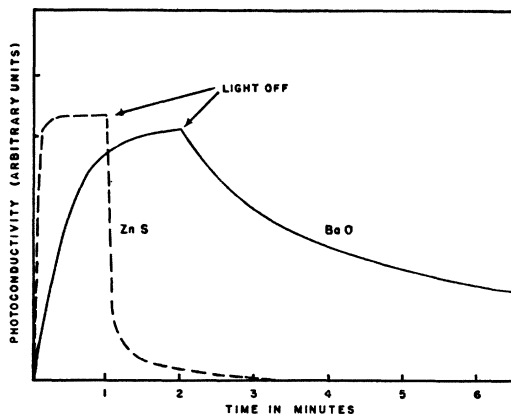


FIG. 3. Photoconductivity as a function of time for crystals of BaO and ZnS (sphalerite). Illumination begins at time=0. The current decay in BaO after illumination ceases is approximately exponential.

¹⁰ W. W. Tyler, *Phys. Rev.* **76**, 179 (1949).

¹¹ F. C. Nix, *Revs. Modern Phys.* **4**, 723 (1932)

about $0.5 \text{ mm} \times 0.5 \text{ mm} \times 0.5 \text{ mm}$. The hydrogen arc and Bausch and Lomb monochromator were used to provide monochromatic radiation. Photocurrents were measured using a parallel-balanced electrometer circuit employing two Victoreen VX-41 input tubes. Currents of the order of 10^{-14} amp could be detected. The dc measurements were made at room temperature.

Initial studies were made on six different crystals from three different crystallizing runs. For all the samples, appreciable photocurrents were measured from 3300A to 2100A. The dc measurements are characterized by the superposition of photocurrents on dark currents of comparable magnitude and by the long times required to obtain equilibrium current values. Figure 3 shows a recorder trace of current *vs* time for a BaO crystal during a two-minute exposure to 3000A light and after the light is removed. A similar measurement is shown for a zinc sulfide (sphalerite) crystal. This time effect in BaO was independent of the particular

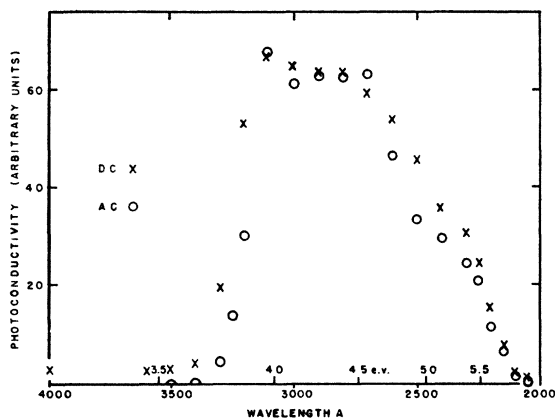


FIG. 4. Photoconductivity as a function of wavelength. The illumination spectrum is given in Fig. 7. The dc data are for crystal No. 6; the ac data are for crystal No. 7.

crystal studied and was observed in all regions of the spectrum in which photoconductivity was observed. The exceptionally long time effect is probably not caused by a change in the semiconduction current due to heating by the incident light, since the observed time required to attain constant currents is greater by a factor of about 100 than the approximate calculated time necessary for thermal equilibrium to be established. The exponential decay after removal of the light may be due to the thermal release of trapped electrons. However, no studies of the time effect as a function of the crystal temperature were undertaken. (No detectable time effects could be observed using the ac detection method described below.)

Figure 4 shows the wavelength dependence of the dc photoconductivity in BaO. Measurements for a different crystal using the ac detection system are shown for comparison. Both curves represent room temperature photocurrents, uncorrected for spectral variations in intensity of the light source. The dc data represent

approximate steady-state values, taken 2 minutes after exposure, with time allowed for complete recovery between readings. Ordinates for the two curves are arbitrarily matched. Except for the long wavelength "tail" on the dc curve, the wavelength dependence for the two methods agrees within experimental error. The higher the impurity content of the crystal, the larger the dark current observed with dc detection. In some cases (e.g., crystal No. 7 of Fig. 4, 0.05 percent molybdenum), large concentrations of impurities precluded dc photoconductivity measurements.

The dc system was checked by observing photoconductivity in small crystals of zinc sulfide (sphalerite) and diamond. The results indicate approximate agreement with published data^{12,13} taken using ballistic techniques. Several attempts were made to observe photoconductivity in crystals of MgO. Although MgO absorbs appreciably between 2500A and 2000A (Fig. 1), no photoconductivity could be detected at any wavelength in this region.

B. Alternating Current Measurements

1. Experimental Details

To avoid the complications of dark currents and time effects in subsequent photoconductivity measurements, the light falling on the crystal was square-wave modulated by a rotating shutter, and the resultant ac component of current through the crystal was measured. Figure 5 shows a diagram of the experimental arrangement. Light from the hydrogen arc is chopped into 33 square pulses per second, is dispersed by the monochromator, and falls on the BaO crystal in the vacuum. A dc voltage is maintained across the crystal, and ac current components are coupled to the preamplifier through the capacitor *C* ($0.05 \mu\text{f}$). After amplification the signal goes to the phase-sensitive detector which rectifies and detects only ac voltages in synchronism with an auxiliary signal generated by the phototube on the periphery of the chopper disk. Control of the relative phases of the two signals is obtained by moving the phototube along the periphery of the disk. The use of phase-sensitive detection gives a convenient and stable method of attaining a narrow band-pass and consequent high signal-to-noise ratio.

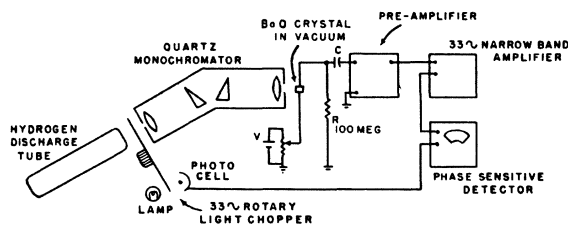


FIG. 5. Diagram of ac photoconductivity apparatus. The input impedance of the preamplifier is a resistance of 2000 megohms; *C* is $0.05 \mu\text{f}$. For other details, see text.

¹² B. Gudden and R. W. Pohl, *Z. Physik* 17, 331 (1923).

¹³ B. Gudden and R. W. Pohl, *Z. Physik* 3, 123 (1920).

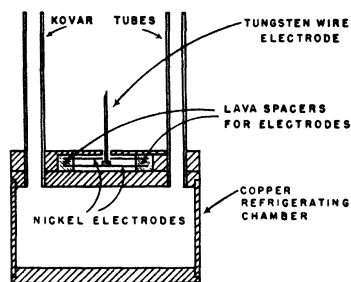


FIG. 6. Crystal mount for photoconductivity measurements as a function of temperature. The "tungsten wire electrode" is a 0.003-in. tungsten wire connecting to a 0.050-in. oxidized tungsten rod, 0.020-in. long, which is pressed onto the upper surface of the crystal by a light coil spring and glass support. The crystal lies between this rod and the lower nickel electrode.

The preamplifier consists of two parallel-balanced Victoreen VX-41 electrometer tubes which are battery powered and spring suspended to minimize the effects of microphonics. It is essentially an impedance transformer, having a voltage gain of about one-half. The basic design of the narrow band parallel-balanced amplifier is largely due to Roess,¹⁴ who has presented a good discussion of the problems involved in building low frequency narrow band amplifiers. Phase-sensitive detection is obtained by connecting each phase of the "push-pull" output from the amplifier to one of the grids of a 6SL7; the cathodes are tied together and driven by the auxiliary phase signal. A microammeter and *RC* circuit with a time constant of about 1 second are connected between the plates of the 6SL7.

The 20-db down band width of amplifier and detector is about one cycle, with the maximum gain at 33 cps. The relative response at 60 cps is at least 60 db below the maximum, and no trouble is experienced with 60-cycle "pick-up." At 33 cps with maximum gain, full-scale deflection of the output meter represents 2×10^{-6} v rms at the input of the preamplifier. The noise level for the system with preamplifier and 100-megohm input resistor, but without the BaO crystal, is about 7×10^{-7} v. Output readings are approximately linear over an 80-db range of input voltage. Actually, the limitation on the magnitude of minimum photocurrents detectable is due to noise in the dark current of the BaO crystals. Currents measured for the data shown below were of the order of 10^{-14} to 10^{-12} ampere, with signal to noise ratios of the order of 10 to 1000.

The crystal mount used for ac photoconductivity measurements was designed to allow measurements from room temperature to near liquid nitrogen temperatures. Figure 6 shows the crystal mount, electrodes, and refrigerating chamber. The nickel electrode on which the crystal rests is held at a positive dc potential

with respect to ground; the parallel nickel electrode above the crystal is at ground potential. Through a hole in the top electrode, a tungsten electrode is spring loaded on the crystal. To increase the thermal isolation of the sample, the small tungsten electrode is sealed to a glass rod and welded to a 0.003-in. wire which runs through the glass rod and through a Kovar-glass seal in the vacuum head to the input of the preamplifier. Thick copper plates above the electrodes and crystal are attached to the refrigerating chamber and serve to maintain the temperature of crystal and electrodes at approximately the temperature of the chamber. A copper-constantan thermocouple attached to the top electrode just above the crystal is used for temperature measurements. With liquid nitrogen in the cylinder, the lowest temperature recorded was -180°C . The crystal temperature is estimated to be within 5° of the electrode temperature.

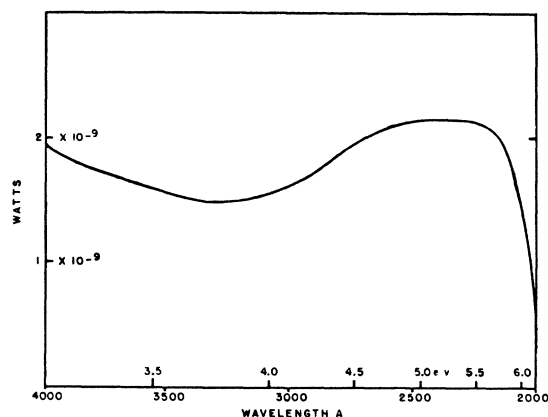


FIG. 7. Spectral energy distribution for light source and monochromator. The source is a Hanovia No. 71-3 hydrogen discharge tube in a quartz envelope operated at 3000 v ac, 0.3 amp. The Bausch and Lomb quartz monochromator is used with a constant width of both slits of 0.5 mm. The energy is determined by an RCA Cs-Sb phototube C-7120 calibrated against a thermopile.

The light source used for most of the measurements of both optical absorption and photoconductivity is a quartz, water-cooled, hydrogen discharge tube¹⁵ similar to one described by Kistiakowsky.¹⁶ The spectral energy distribution for this lamp is shown in Fig. 7. Due to the low light level, this calibration could not be obtained directly using a vacuum thermopile. Instead, a Cs-Sb phototube with a quartz window¹⁷ was calibrated against the thermopile at high light levels using a high pressure mercury arc for light source. The sensitivity of the electrometer circuit used with the phototube was then increased by a factor of 10^3 and the hydrogen arc calibrated against the phototube. The error in relative values of the spectral distribution is probably less than 5 percent. The errors in absolute energy values are dif-

¹⁴ L. C. Roess, *Rev. Sci. Instr.* **16**, 172 (1945). We are indebted to Dr. H. B. DeVore, RCA Laboratories, Princeton, New Jersey, for valuable discussions of problems relating to low frequency narrow band amplifiers.

¹⁵ Hanovia Chemical and Manufacturing Company, No. 71-3.

¹⁶ G. B. Kistiakowsky, *Rev. Sci. Instr.* **2**, 549 (1931).

¹⁷ We are indebted to Dr. R. W. Engstrom, RCA Tube Division, Lancaster, Pennsylvania, for supplying us with this tube.

difficult to estimate and may be as much as 50 percent. The single crystals used in the ac experiments were about 1 mm×1 mm×1 mm.

2. Experimental Results

The lower curve, Fig. 8, shows the photoconduction current as a function of wavelength. The upper curve represents the same data normalized to a constant number of photons per second in each wavelength interval, using the spectral energy distribution shown in Fig. 7. The correction of the data changes the shape of the curve so slightly that the data below are presented without this normalization. The absolute magnitude of the quantum efficiency is difficult to estimate because of lack of knowledge of the mean range of the charge carriers. The ordinates in Fig. 8 are calculated on the assumption that the carriers freed by photon absorption remain free until striking an electrode. The ordinates thus represent lower limits for the quantum efficiency. At 4.0 eV, the quantum efficiency is greater than 5×10^{-2} and probably of the order of unity. (Evidence presented below in connection with Fig. 12 will show that the quantum efficiency probably appreciably exceeds the lower limit given by Fig. 8.)

The general shape of the curves showing photoconductivity plotted against wavelength is the same for seven crystals studied, taken from three different crystallizing runs, and containing varying amounts of impurities.¹⁸ For the photoconductivity data the

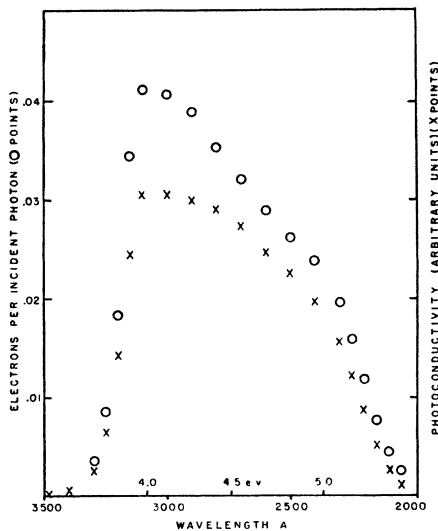


FIG. 8. Correction of data to constant number of photons incident per second at each wavelength. The crosses are the original data on BaO crystal No. 9. The circles are the data corrected by using Fig. 7. The quantity "electrons per incident photon" is intended only as a lower limit to the quantum efficiency, since the electric field was not large enough to give saturation currents.

¹⁸ As mentioned in footnote 4, the principal features of the observed wavelength dependence of both optical absorption and photoconductivity are believed to be intrinsic to the BaO lattice. However, using the larger crystals of higher purity, only recently available, and employing greater resolution, the slight peak in

monochromator slit width was 0.5 mm, giving resolution of about 80Å at 3000Å. Within this resolution, the threshold for photoconductivity was coincident with that for absorption for all the crystals studied. Figure 9 shows thresholds for photoconductivity and absorbance plotted for two crystals from the same crystallizing run. Due to the fact that all crystal samples used were exposed to the atmosphere for a short time, while being transferred from the dry box to the vacuum, one might expect that the data shown in Fig. 9 are characteristic of a film of Ba(OH)₂ which must form on the BaO crystal surfaces. However, Ba(OH)₂ does not absorb appreciably anywhere in the region from 4000Å to 2000Å. This was convincingly demonstrated during the film study⁸ by observation of the transmittance of BaO films as they were converted to Ba(OH)₂ films.

Although the optical absorption in BaO is quite insensitive to temperature change,⁸ the magnitude of photoconduction currents is quite sensitive to temperature. Figure 10 shows photoconductivity as a function of wavelength for several temperatures. The shape of the wavelength dependence is the same at each temperature investigated. Crystals with different im-

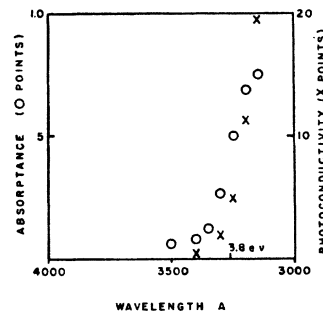


FIG. 9. Comparison of thresholds for absorbance and photoconductivity of a BaO crystal.

purity content show different temperature dependence, the purer crystals showing detectable photoconductivity at lower temperatures. Figure 11 shows temperature dependence of photoconductivity at fixed wavelength and fixed field strength for two crystals, No. 9 and No. 11. Crystal No. 9 contains about 0.05 percent Mo in addition to Sr and Ca impurities; crystal No. 11 is relatively free of Mo. Photoconductivity could not be observed below -120°C for any of the crystals studied. The peak in the temperature dependence of photoconductivity shown for crystal No. 11 at -10°C has been observed for only two samples and is probably not significant.

It should be emphasized that the data shown represent steady-state currents and that the temperature dependence observed is probably not intrinsic to BaO. Lenz,¹⁹ studying steady-state photoconductivity in diamond and zincblende, noted temperature dependence of the same nature as that observed in BaO. As a result

the photoconductivity indicated in Fig. 4 and Fig. 10 at about 4.0 eV appears considerably sharper and higher relative to the rest of the curve.

¹⁹ H. Lenz, Ann. Physik 77, 449 (1925).

of later work using ballistic techniques, Lenz²⁰ attributed this observed temperature dependence in diamond to the temperature dependence of space charge effects. In the present work, a few measurements have been made at liquid air temperatures using the ballistic technique. The signal-to-noise ratio was poor because of the small energy absorbed in each pulse of light, but the experiments serve to confirm the space charge interpretation of the temperature dependence of photoconductivity.

Figure 12 shows photoconductivity as a function of the strength of the dc field across a BaO crystal, for various temperatures. It is apparent that even for fields of the order of 15,000 v per cm there is no evidence for saturation of the photoconduction current. Higher fields cannot be applied because of the abrupt rise of noise in the dark current. The failure to draw saturation currents in any of the crystals studied indicates that

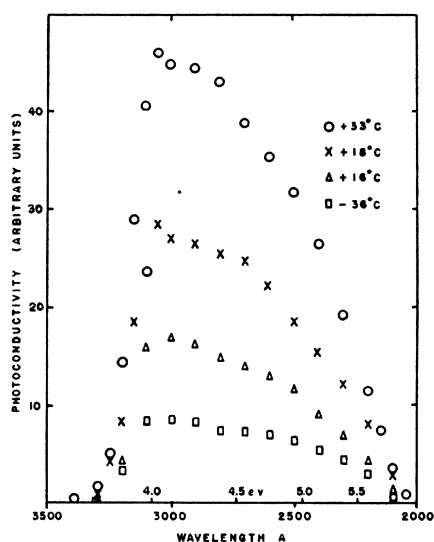


FIG. 10. The ac photoconductivity for BaO crystal No. 9 at various temperatures.

the charge carriers do not remain free until they strike an electrode; therefore, the quantum efficiency computed for Fig. 8 is only a lower limit and the actual quantum efficiency is considerably larger.

Like the temperature dependence, the field dependence of photoconductivity is impurity sensitive. Curves of the type shown in Fig. 12 are in general slightly concave upward but become more nearly straight lines for the crystals of highest purity. Again this behavior suggests the existence of a large space charge in the crystals of higher impurity concentration, probably due to trapping of photoconduction electrons at impurity centers. Techniques have not yet been developed for the inclusion of controlled amounts of impurity in BaO crystals, and, therefore, no systematic correlation between either temperature dependence or field de-

²⁰ H. Lenz, Ann. Physik 83, 941 (1927).

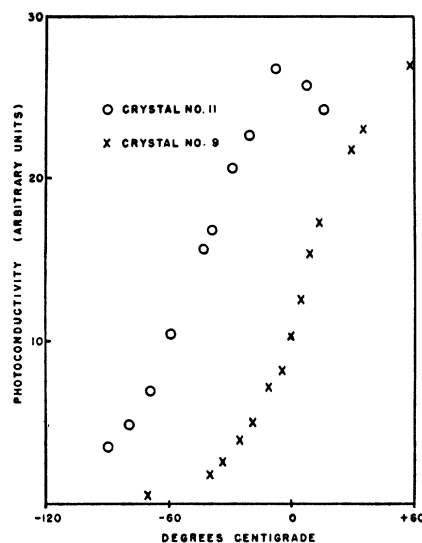


FIG. 11. The ac photoconductivity as a function of temperature. The wavelength in both cases is 3000Å, and the potential difference across the crystals (each about $\frac{1}{2}$ mm thick) is 500 v. Crystal No. 11 is of higher purity.

pendence of photoconductivity and impurity content can be presented.

The crystal mount used for the above measurements was designed to minimize the effect of external photoelectric currents. However, the field dependence and temperature dependence described above constitute the best evidence that the currents measured in this work are true photoconductivity currents. The currents are so small that the smallest fields used would collect all electrons released by the external photoelectric effect. Furthermore, there is no reason to believe that external photoelectric currents should disappear at low temperatures.²¹

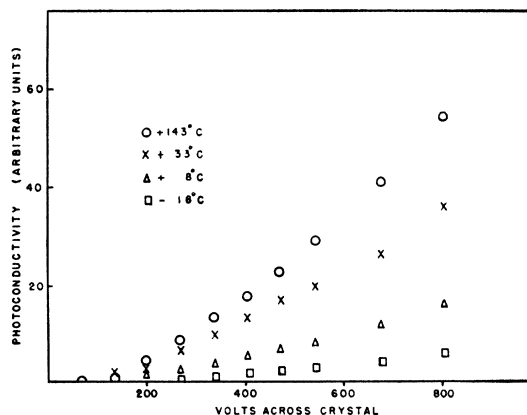


FIG. 12. The ac photoconductivity as a function of electric field strength at various temperatures. The BaO crystal is No. 8, 0.56 mm thick in the direction of the field. Illumination is by a medium pressure mercury arc at 3140Å.

²¹ Using a 1000-watt H-6 Hg arc as light source, photocurrents could be measured from BaO crystals at any strong Hg line in the visible region of the spectrum. The quantum efficiency for this

Attempts were made to measure photoconductivity in evaporated BaO films simultaneously with absorption measurements. The dc electrometer was used for this measurement. Films were evaporated⁸ on a quartz plate on which platinum electrodes had been coated. The electrodes were each 1 cm long and were separated by 1 mm. After deposition of the film, dark currents of the order of 10^{-11} amp were observed at room temperature with 67 v dc across the film. The dark currents were not linear with film thickness or stable with time. No photocurrents could be observed superimposed on the large dark current. On decreasing the temperature of the film to -150°C , the dark currents became negligible ($<10^{-14}$ amp), and photocurrents of the order of 5×10^{-14} amp were observed from about 3100A to 2500A. The total light intensity absorbed in the film was greater than that absorbed during the single crystal measurements. Film photocurrents were independent of voltage between electrodes for voltages above 200. The very small magnitude of film currents and the independence of field strength probably indicate that the film is made up of very small crystals, with interfaces between these crystals decreasing the mobility of charge carriers. The large room temperature dark currents are probably due to surface and interface semiconduction in the film. The presence of detectable photocurrents in films at -150°C is consistent with the fact that the temperature dependence of photoconductivity observed in single crystals is not intrinsic.

V. CONCLUSIONS

A detailed interpretation of these experiments will not be attempted here. The experimental conclusions and a brief analyses of their relation to other experiments and to the properties of BaO follow.

1. The fundamental optical absorption band begins at a photon energy of about 3.8 ev. The band edge has been located by measurements on both crystals and evaporated films. The evidence for the fundamental nature of the band comes from the invariance of the absorption spectrum with impurity content of crystals and with irradiation history, and, principally, from the magnitude of the absorption constant ($>10^5 \text{ cm}^{-1}$). This absorption occurs at a much lower photon energy than estimates²² based on x-ray data for similar oxides would indicate.

2. The threshold for optical absorption is insensitive to temperature in the region -150°C to $+30^{\circ}\text{C}$. No systematic motion of this threshold has been observed under conditions where a 0.02-ev displacement could be detected. The magnitude of the average change in minimum energy for this excitation process is therefore less than $10^{-4} \text{ ev}/^{\circ}\text{C}$ in this temperature range.

photoeffect is less than for photoconductivity currents from 3300A to 2100A by a factor of at least 10^2 . These photocurrents did not disappear at -180°C and may be external photoelectric currents. Using the lower intensity hydrogen arc source, no currents were detectable except the photoconduction currents in the region of strong optical absorption.

²² N. F. Mott and R. W. Gurney, reference 2, pp. 76-78, 101.

3. The threshold for photoconduction occurs at the same energy as for optical absorption. This statement applies to photoconduction with quantum efficiency of the order of 0.01 or more. Small photoelectric or photoconduction currents are observed at longer wavelengths, but these have not been investigated in detail; the optical absorption constant is so small in this region that impurities or *F*-centers probably provide the electrons.

4. A second rise in the optical absorption begins at about 4.8 ± 0.2 ev. At this energy the photoconductivity is decreasing with increasing photon energy. Such behavior has been ascribed²³ to limitation of photoconduction currents by recombination when the absorption of light takes place in a very thin layer at the surface of a crystal. Such an explanation does not appear reasonable in the present problem for two reasons: (a) The absorption constants at 4.5 and 5.2 ev are the same, but photoconductivities differ by greater than a factor of two; (b) A rough quantitative theory of the variation of recombination rate with absorption constant predicts that the photoconductivity would fall toward zero much less rapidly than the observations indicate. (The data show a decrease of more than a factor of 100 from 4.1 to 6.2 ev.) It should be observed that the above considerations are based on the assumption of a perfect crystal, neglecting the possibility that the quantum efficiency for production of free charge may depend on the distance from the surface at which photon absorption takes place.

It appears quite possible that two different excitation processes could be causing the optical absorption. (The absorption edge is perhaps due to exciton production, with the second rise due to band-to-band transitions.) One would have a threshold energy of 3.8 ev, a peak at 4.1 ev, and it would fall slowly to nearly zero at 6.2 ev; this absorption would be accompanied by photoconductivity. The second process would have a threshold at about 4.8 ± 0.2 ev and would not be accompanied by photoconductivity of comparable quantum efficiency. However, we know of no proposed explanation for an absorption process unaccompanied by photoconductivity at higher energy than the photoconduction threshold.

5. The magnitude of the photoconduction current is a sensitive function of temperature, a function of impurity content, and a nonlinear function of the applied electric field. In each case the dependence is such that the existence of space charge in the crystal is suggested. The positive holes left in the filled band after the excitation of electrons may or may not be mobile. If mobile, they may be trapped, and then the rate of release from traps would be an exponential function of temperature. The same statement applied to the excited electrons. Except for the possibility of recombination or complete transit of the crystal, any motion of electrons and holes

²³ N. F. Mott and R. W. Gurney, reference 2, p. 104.

results in a space charge reduction of the field in the crystal. Since the electrons are probably more mobile than the holes, the temperature dependence of photoconductivity probably represents the variation with temperature of the rate of release of electrons from traps.

6. The excitation process responsible for the observed light absorption may be either the creation of a free electron and hole or the creation of an exciton. Mott²⁴ has attributed the first (lowest energy) fundamental absorption bands in the alkali halides to exciton creation. Such excitons in BaO would probably be thermally dissociated at room temperature.²⁵ The present experiments cannot distinguish between a band-to-band electronic transition, which enables an electron to move

²⁴ N. F. Mott, *Trans. Faraday Soc.* **34**, 500 (1938).

²⁵ Mott has estimated in *Proc. Phys. Soc. (London)* **A167**, 384 (1938), the extent to which dissociation of excitons may contribute to photoconductivity. If one inserts the value 4 for the optical dielectric constant and 34 for the static dielectric constant (recently measured in this laboratory) into Mott's estimation (p. 390), one finds that temperatures much below liquid air temperature would be required to prevent dissociation of excitons in BaO. This contrasts with the behavior of NaCl, which has a lower dielectric constant and in which optical absorption without photoconductivity has been observed at room temperature by Ferguson (*Phys. Rev.* **66**, 220 (1944)).

freely immediately after the absorption of light, and a transition to an exciton state, which would be quickly dissociated to yield an electron moving freely. Experiments with single, short light pulses (to reduce the effects of space charge) should be performed down to liquid hydrogen temperatures to distinguish between these processes.

Another way in which photoconductivity could result from the creation of excitons has recently been demonstrated by Apker and Taft.²⁶ They showed that excitons produced by absorption in the first fundamental absorption band in KI may ionize *F*-centers, giving rise to electrons in the conduction band. Such a process may contribute to photoconductivity in BaO, competing with thermal dissociation of excitons in the production of conduction electrons.

VI. ACKNOWLEDGMENTS

The authors are indebted to Dr. Arnold R. Moore and Mr. S. S. Stevens for valuable assistance in this work and are especially grateful for many discussions with Professor J. A. Krumhansl on the interpretation of these experiments.

²⁶ L. Apker and E. Taft, *Phys. Rev.* **79**, 964 (1950).

Low Energy Photomeson Production in Hydrogen

S. D. DRELL

Stanford University, Stanford, California

(Received February 8, 1951)

Berkeley experiments have revealed the general features of the neutral and charged π -meson photoproduction cross sections for gamma-rays incident on protons. In particular, approximate equality of the π^0 and π^+ production cross sections has been observed. This has proved difficult to account for theoretically. Calculations based on a weak coupling perturbation treatment of the meson-nucleon interaction predict the π^0 production to be reduced by $\sim(\mu/M)^2$ relative to π^+ production for energies at which the Berkeley experiments are performed (~ 320 Mev). In this paper we avoid the perturbation theory approximation of weak nucleon-meson coupling. By means of a canonical transformation of the type introduced by Bloch and Nordsieck, we obtain a solution to the hamiltonian equation that involves no assumption concerning the largeness or smallness of $g^2/4\pi$. The

approximations involved are neglect of nucleon recoil and treatment of spin and charge matrices as classical unit vectors. Handling the electromagnetic field by standard perturbation theory, we use this solution to calculate the matrix elements for photoproduction. In evaluating the matrix elements we must use a finite source cutoff to compensate neglect of nucleon recoil. We obtain qualitative agreement with the observed equality of π^0 and π^+ production cross sections with a choice of $g^2/4\pi \sim 1-2$ and of source radius of the order of a nucleon Compton wavelength. Calculation of the anomalous nucleon magnetic moments corroborates a choice of these constants in this range. We also obtain an angular distribution and energy dependence for the production cross sections in accord with observation.

I. INTRODUCTION

EXTENSIVE experimental work at Berkeley has established the following general features of the photomeson production process, for gamma-rays of energy up to 320 Mev incident on protons:

1. The cross sections for production of neutral and charged pi-mesons by 320-Mev bremsstrahlung are approximately equal, ($\sigma_T \sim 10^{-28}$ cm²).^{1,*}

¹ Steinberger, Panofsky, and Steller, *Phys. Rev.* **78**, 802 (1950). J. S. Steller and W. K. H. Panofsky, *Phys. Rev.* **81**, 649 (1951). I wish to thank Professor R. Serber for calling my attention to this result.

* Note added in proof.—Later data indicate a reduction in π^0 production by a factor of roughly three relative to π^+ production.

2. The production cross sections are approximately isotropic in the center-of-mass frame.²

3. The excitation function for the production of neutral mesons is steeper than for the production of charged mesons.³

This paper attempts to arrive at an understanding of these features of neutral and charged photomeson production within the framework of the present formulation of meson field theory. From the point of view of

² Steinberger, Panofsky, and Steller, *Phys. Rev.* **78**, 802 (1950); K. A. Brueckner, *Phys. Rev.* **79**, 641 (1950) (see p. 645).

³ J. S. Steller and W. K. H. Panofsky, *Phys. Rev.* **81**, 649 (1951); J. Steinberger and A. Bishop, *Phys. Rev.* **78**, 494 (1950).